ELSEVIER

Journal of Controlled Release 62 (1999) 109–114

journal of controlled release

www.elsevier.com/locate/jconrel

New biodegradable polymers for injectable drug delivery systems

B. Jeong[a], Y.K. Choi[a], Y.H. Bae[a], G. Zentner[b], S.W. Kim[a,*]

[a]*Department of Pharmaceutics and Pharmaceutical Chemistry, Center for Controlled Chemical Delivery, University of Utah, Salt Lake City, UT 84112, USA*

[b]*MacroMed, Inc., 419 Wakara Way, Suite 205, Salt Lake City, UT 84108, USA*

Abstract

Many biodegradable polymers were used for drug delivery and some are successful for human application. There remains fabrication problems, such as difficult processability and limited organic solvent and irreproducible drug release kinetics. New star-shaped block copolymers, of which the typical molecular architecture is presented, results from their distinct solution properties, thermal properties and morphology. Their unique physical properties are due to the three-dimensional, hyperbranched molecular architecture and influence microsphere fabrication, drug release and degradation profiles. We recently synthesized thermosensitive biodegradable hydrogel consisting of polyethylene oxide and poly(L-lactic acid). Aqueous solution of these copolymers with proper combination of molecular weights exhibit temperature-dependent reversible sol-gel transition. Desired molecular arrangements provide unique behavior that sol (at low temperature) form gel (at body temperature). The use of these two biodegradable polymers have great advantages for sustained injectable drug delivery systems. The formulation is simple, which is totally free of organic solvent. In sol or aqueous solution state of this polymer solubilized hydrophobic drugs prior to form gel matrix.

1. Introduction

Over the past two decades extensive research has been performed in the design of polymeric drug delivery systems [1,2]. Among them, the use of biodegradable polymers has been successfully carried out. They include polyesters [3–5], poly(orthoesters) [6], polyanhydrides [7,8], polyamino acid [9,10], poly(alkyl cyanoacrylates) [11], polyphophazenes [12,13], copolymers of (PLA/PGA) and asparate [14] or PEO [15].

Although these biodegradables were used for drug delivery and some are successful for human application, there remains fabrication problems, difficult processability and limited organic solvent and irreproducible drug release kinetics. In this paper, two new approaches for the design of biodegradable polymers and drug delivery are discussed.

2. Star-shaped PEO–PLA block copolymers

A new series of thermoplastic biodegradable hydrogels (TBH) based on star-shaped poly(ether-ester) block copolymers have been synthesized in this laboratory [16]. Physically crosslinked TBH may present improved biocompatability, mass transport, biodegradability, and processability, and thus can provide a better way of parenteral injectable drug delivery (Fig. 1).

*Corresponding author.

0168-3659/99/$ – see front matter
PII: S0168-3659(99)00061-9

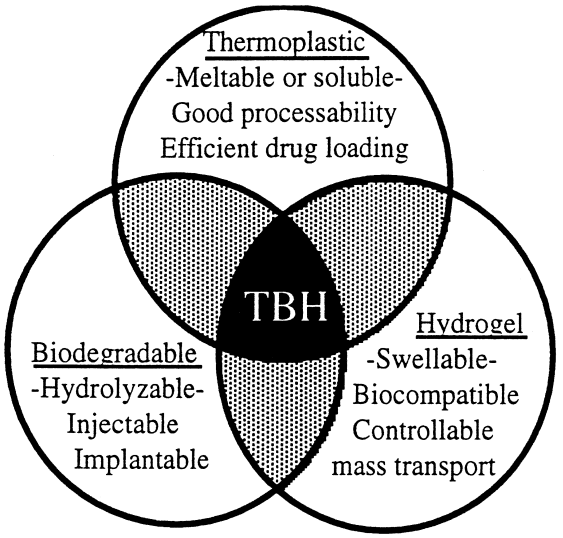

Fig. 1. Schematic illustration of TBH.

New star-shaped block copolymers, of which the typical molecular architecture is presented, result from their distinct solution properties, thermal properties and morphology.

Table 1 summarizes the advantages of star-shaped PEO–PLA and PEO–PCL block copolymers over current biodegradable polymers, which are derived from consideration of hydrogel character, thermoplastic property, biodegradability, based on molecular architecture. A broad spectrum of performance characteristics can be easily obtained by manipulation of various comonomers, number of arms, polymer composition, and polymer molecular weight. Fig. 2 is the schematic illustration of how these parameters can influence the drug delivery application. It is expected that three main parameters such as polymer composition, molecular weight, and number of arms will affect the physical properties of block polymers involving swelling, solution, and thermal behaviors. Special concerns are listed in each box representing physical properties in Fig. 2. Subsequently, physical properties will have an effect on the delivery system, thus eventually determining the formulation process and in vivo fate of polymers and degradation by-products. We investigated the correlation between polymer structure, physical properties of polymers, and a microsphere protein delivery system. Four types of star-shaped block copolymers were prepared by ring opening polymerization of L-lactide and ε-caprolactone initiated by star-shaped PEOs.

Their unique physical properties are due to the three-dimensional, hyperbranched molecular ar-

Table 1
The advantages of proposed star-shaped PEO–PLA and PEO–PCL block copolymers

1	Biocompatible due to imbibed water and nontoxicity of the polymer
2	Minimum mechanical irritation due to flexibility and softness
3	Biodegradable via simple hydrolysis or enzymatic reactions (implantable and injectable)
4	Controllable degradation rate
5	Control of drug release rate and duration Diffusion and degradation controlled
6	Improvement in drug release kinetics Reduced burst effect No multiphasic release pattern
7	Synthesis separated from processing No chemical reaction during fabrication Ability to obtain high purity of polymers
8	Proper mechanical strength in swollen state
9	Good mass transport (permeable to macromolecules)
10	Efficient drug loading scheme
11	Diverse processing due to broad solubility and low melting temperature: (i) Solution processing: solvent casting, dipping, spraying (ii) Hot melt methods: extrusion, injection molding, calendering, blow molding (iii) Other methods: nano- and microencapsulation, micellization
12	No limit in fabrication of various dosage forms
13	Easy sterilization

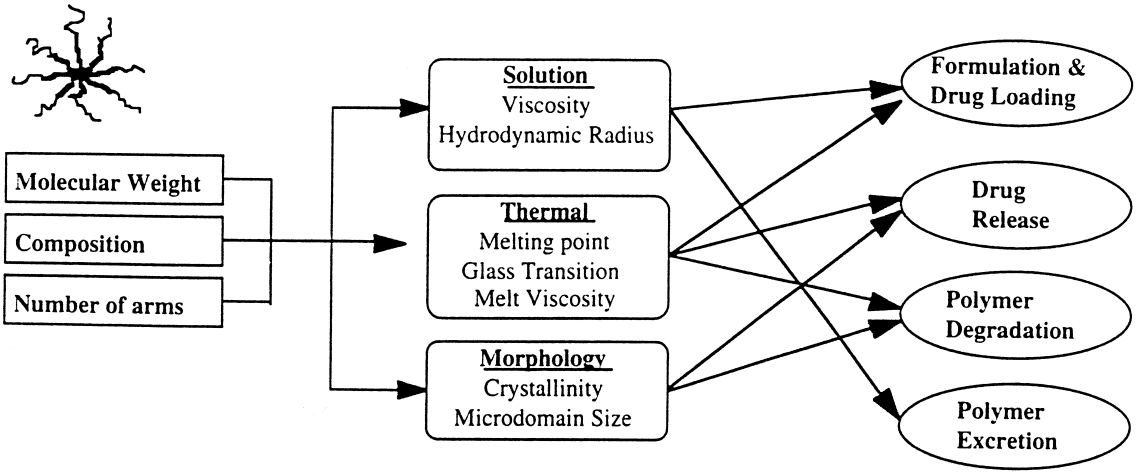

Fig. 2. Design and application of star-shape block copolymers.

chitecture and may influence microsphere fabrication, drug release and degradation profiles. We studied albumin (BSA: a model protein) loaded microspheres prepared from star-shaped poly-(ethylene oxide) (PEO)-poly(L-lactic acid) (PLA) block copolymers. The molecular architecture effects on microsphere preparation, polymer degradation and drug release were studied.

In vitro BSA release profiles showed a close correlation with the degradation profiles. The initial phase (the first 25 days) showed no significant difference between star-polymers. Interestingly, no drug burst was observed in all cases. However, in the latter phase, 8-arm PEO–PLA showed an increase in BSA release rate, while 2- and 3-arm PEO–PLA showed decline. Four-arm PEO–PLA showed an in-between release pattern, demonstrating almost zero-order release kinetics.

Architectural modification of degradable polymers by branching resulted in a significant effect on degradation and drug release profiles, due to the differences in chain length, crystallinity, and morphology. Polymer branching caused accelerated degradation, especially in the latter phase, and thus afforded a more favorable release profile. Star-shaped PEO exhibits a smaller hydrodynamic radius when compared to the linear one of the same molecular weight. Since PEO is non-biodegradable and has an extraordinarily large hydrodynamic radius, it is advantageous to use a PEO having smaller molecular dimension for easy renal excretion after use.

3. Thermosensitive biodegradable block copolymers

Most previous works on thermosensitive polymers included only non-degradable smart polymers. Recently new series of biodegradable triblock copolymers were designed. The polymer consists of poly-(ethylene glycol)–poly(DL-lactic acid-co-glycolic acid)–poly(ethylene glycol) (PEG–PLGA–PEG). Molecular architecture by hydrophobic/hydrophilic balance and arrangement of different molecular weights are important factors for obtaining materials which show sol-gel transition depending on temperature changes [17]. When low molecular weight of PEG vs. high molecular weight of PLGA was used, the aqueous solution of PEG–PLGA–PEG triblock copolymer forms a solution at room temperature while it becomes a gel at body temperature within a few seconds. Further increase in temperature makes the gel opaque with gel-sol transition phenomena (Fig. 3). The triblock copolymer was synthesized by ring opening polymerization of DL-lactide and glycolide onto monomethoxy poly(ethylene glycol) using stannous octoate as a catalyst, followed by coupling with 1,6-hexamethylene diisocyanate. The structure of synthesized polymer is as follows:

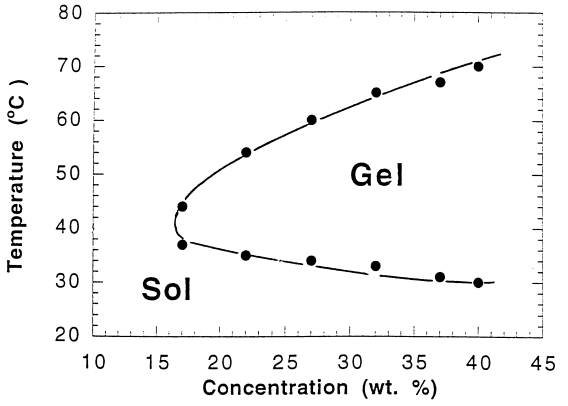

Fig. 3. Phase diagram of PEG–PLGA–PEG triblock copolymer aqueous solutions. Sol (flow) to gel (no flow) transition temperature was measured by test tube inverting method increasing 2°C/step. The sample solution was equilibrated for 15 min at setting temperature before the measurement at each step. The transition temperature was so sharp and was determined within ±1°C.

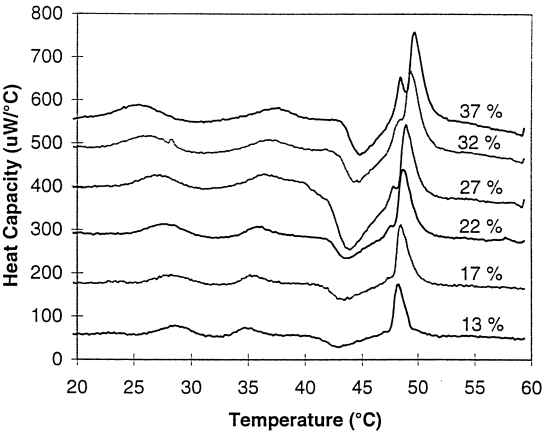

Fig. 4. DSC thermogram of PEG–PLGA–PEG triblock copolymer aqueous solutions. The thermogram was obtained while heating with the heating rate of 1°C/min.

$$CH_3O\underset{PEG}{[CH_2CH_2O]_x}\{\underset{PLGA}{[COCH_2O]_y[COCH(CH_3)O]_z}\}$$

$$CONH(CH)_6NHCO\{\underset{PLGA}{[OCOCH_2]_y[OCOCH(CH_3)]_z}\}$$
Urethane linkage

$$\underset{PEG}{[OCH_2CH_2]_x}OCH_3$$

Fig. 3 shows a phase diagram of an aqueous solution of the PEG–PLGA–PEG (550–2810–550 where DL-lactic acid/glycolic acid ratio is 78/22 by weight, determined by ^{1}H-NMR, $M_w = 4395$, $M_w/M_n = 1.22$ by gel permeation chromatography) triblock copolymer. At room temperature, relative viscosity of the 32 wt.% aqueous solution to distilled water determined by Cannon–Fenske viscometer is 10, which is good for injection of the solution using a 22 gauge syringe. With increased temperature, the solution undergoes sol to gel transition. Further increase in temperature makes the transparent gel opaque, disturbed the gel integrity to flow at higher temperature (gel to sol transition), and finally polymers were macroscopically phase separated from water.

Differential scanning calorimeter (DSC) thermogram (Fig. 4) of triblock copolymer aqueous solutions shows two maxima and one first order transition. The first order transition (ΔH(exotherm) = −136.94 kJ/g polymer) occurs at 48°C irrespective of concentration in the range of 13% to 42%. This temperature may be related to phase transition of the gel. The first maximum in the thermogram correlates to sol to gel transition (lower temperature boundary). With increasing polymer concentration, this transition shifted to a lower temperature. At a concentration less than 15%, the solution became a turbid sol at high temperature but no gel formed. This indicates there is a critical gel concentration (CGC). For this polymer, CGC is about 16% by weight. The second maximum may be related to opaque gel formation. The processes characterized as heat capacity maximum are widely discussed in protein folding as evidence of hydrophobic interactions. As shown in Fig. 4, the temperature range of the transparent gel region at ~35°C became broader with increasing concentration. There is a discrepancy between the transition temperature observed in the DSC experiment and that observed in the phase diagram. This could result from the different experimental methods used to determine the transition temperature. In the DSC experiment, the temperature was increased 1°C/min; while to construct the phase diagram, the solution was equilibrated for 15 min at each evaluated temperature. If there was no flow when the vials were inverted, it was regarded as a gel [18]. To cause the gel to flow, an approximate shear stress of 65 Pa is needed [19].

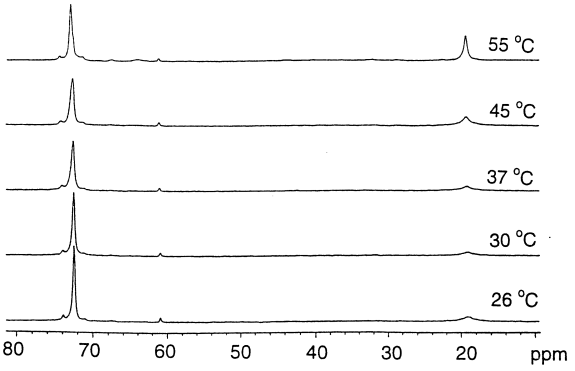

Fig. 5. ^{13}C-NMR (500 MHz) spectra of 27% (wt.) PEG–PLGA–PEG triblock copolymer in D_2O. The sample was equilibrated for 15 min at setting temperature before measurement; 26°C (sol phase), 30°C (sol to gel transition), 37°C (gel phase), 45°C (turbid gel phase), 55°C (gel to sol transition).

^{13}C-NMR spectra (Fig. 5) in D_2O showed the core-shell structure of the polymer in water. The peak height of the CH_3 peak (18 ppm) from the hydrophobic PLGA relative to hydrophilic PEO (75 ppm) was collapsed and broadened in D_2O at 26°C (sol phase). During sol to gel transition (30°C) and in a gel phase (37°C), these characteristics of the NMR spectra were preserved and this may indicate maintenence of the core-shell structure during the transition. This coincides with the results obtained from the transmission electron microscope (TEM). The TEM picture of a gel phase, formed by dropping 27 wt.% solution onto a gold grid and partial drying for 24 h at 32°C, showed spherical micellar structures with diameters of 10–15 nm. At higher temperatures (45°C and 55°C), the CH_3 peak from PLGA in ^{13}C-NMR spectra increased. This suggests that the core-shell structure of the polymer in an aqueous environment was disturbed due to dehydration of PEO. Phase mixing between PEO and PLGA occurred, resulting in the exposure of the PLGA core phase to aqueous environment. The aqueous solution forms micelles at low concentration which was confirmed by dye solubilization method. Critical micelle concentration (CMC) of the polymer was determined to be about 0.1 wt.% at 25°C.

At room temperature, the micelle is in a dynamic state where there is an equilibrium between unimer and micelles and there seems to be exchange of unimers with the micelles. At increasing temperature, the hydrophobic core is partially dehydrated, causing the micelle to be more rigid. Partial entanglement between micelles maintain the three dimensional structure of the gel. Further increase in temperature disrupts the spherical shape of the micelles, leading to intermicellar fusion followed by macroscopic phase separation of water from the polymer [20].

In conclusion, PEG–PLGA–PEG triblock copolymer aqueous solution showing a sol at room temperature and a gel at body temperature are reported. The gelation mechanism appears to be micellar packing driven by hydrophobic interactions.

Subcutaneously injected sol formed a gel in rat within a few seconds and it was confirmed 24 h after subcutaneous injection of 0.4 ml aqueous solution (33 wt.%) and the integrity of gel remained for more than 1 month (Fig. 6). This property is clearly distinguished from other systems such as Poloxamer™ which is nonbiodegradable and disappeared in 1 day. There was little or no tissue irritation at the injected site even after 1 month [21].

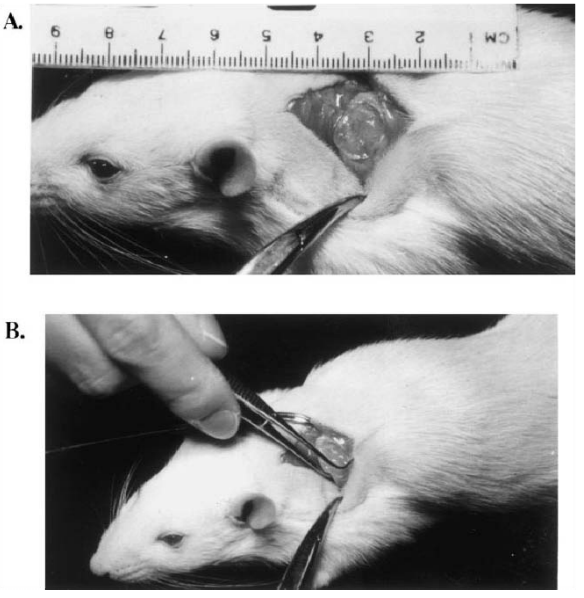

Fig. 6. In situ gel formation after subcutaneous injection of 0.4 ml 33 wt.% copolymers aqueous solution. (A) 24 h after subcutaneous injection, transparent gel was observed. (B) The formed gel retained mechanical property enough to be easily removed using forceps.

Acknowledgements

This work was supported by NIH grant GM56098.

References

[1] S.W. Kim, R.V. Petersen, J. Feijen, in: J. Arien (Ed.), Drug Design, Vol. 5, Academic Press, 1980, p. 193.
[2] R. Langer, N.A. Peppas, Science 263 (1994) 1715.
[3] D.H. Lewis, Drug Pharm. Sci. 45 (1990) 1.
[4] R. Wada, S.H. Hyon, I. Ihada, J. Pharm. Sci. 79 (1990) 919.
[5] H. Okada, M. Yamamoto, T. Heya, Y. Znoue, K. Kanai, Y. Ogawa, G. Toguchi, J. Control. Release 28 (1994) 121.
[6] P. Wuthrich, S.Y. Ng, R.V. Roskos, J. Heller, J. Control. Release 21 (1992) 191.
[7] K.W. Leong, B.C. Blott, R. Langer, J. Biomed. Mater. Res. 19 (1985) 941.
[8] E. Ron, T. Turner, E. Mathiowitz, M. Chasin, M. Hageman, R. Langer, Proc. Natl. Acad. Sci. 90 (1993) 4176.
[9] J.M. Anderson, S.M. Fang, J. Feijen, D. Gregonis, S.W. Kim, Polymer Preprints 20 (1979) 20.
[10] D.B. Bennet, X. Li, N. Adams, C.J.T. Hoes, J. Feijen, S.W. Kim, J. Control. Release 16 (1991) 43.
[11] P. Couvreur, F. Puisieux, Adv. Drug Del. Rev. 10 (1992) 141.
[12] H.R. Allcock, Chem. Eng. News 62 (1985) 22.
[13] S. Cohen, M.C. Bano, K.B. Visscher, M. Chow, H.R. Allcock, R. Langer, J. Am. Chem. Soc. 112 (1990) 783.
[14] G.S. Kwon, M. Yokoyama, T. Okano, Y. Sakurai, K. Kataoka, S. Inoue, J. Control. Release 11 (1990) 269.
[15] L. Youxin, T. Kissel, J. Control. Release 27 (1993) 243.
[16] Y.K. Choi, Y.H. Bae, S.W. Kim, Macromolecules 31 (1998) 8766.
[17] B.M. Jeong, D.S. Lee, Y.H. Bae, S.W. Kim, Nature 388 (1997) 860.
[18] M. Malmsten, B. Lindman, Macromolecules 25 (1992) 5440.
[19] S. Tanodekaew, J. Godward, F. Heatley, C. Booth, Macromol. Chem. Phys. 198 (1997) 3385.
[20] B.M. Jeong, Y.H. Bae, S.W. Kim, J. Colloid Interface Sci., in press.
[21] Private Communication, James Anderson, Case Western Reserve University.